A EUROPEAN JOURNAL

CHEMPHYSCHEM

OF CHEMICAL PHYSICS AND PHYSICAL CHEMISTRY

Table of Contents

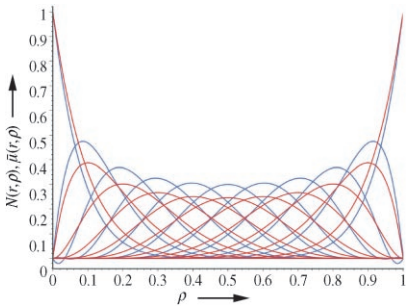

Trading places: Particle distribution and exchange equilibria in a microporous host material are described. Simplified descriptions evolve from the exact formulae in the thermodynamic limit. The authors find that, for example, a single zeolite A nanocrystal consisting of about 1000 "pseudo" unit cells fixes a lower limit for the use of the approximate formula describing the particle distribution. The figure shows the approximate (red) and the exact (blue) particle-distribution dependence on the filling degree between zero and one for a nanocrystal.

WILEY-VCH

DOI: 10.1002/cphc.200500126

Particle Distribution in a Microporous Material: Theoretical Concept

Marc Meyer, Antonio Currao, and Gion Calzaferri*[a]

Particle distribution and exchange equilibria in a microporous host material, built up of equivalent particle sites, which are grouped in larger subsets, are described. Simplified descriptions evolve from the exact formulae in the thermodynamic limit. We find that, for example, a single zeolite A nanocrystal consisting of about 1000 pseudo-unit-cells fixes a lower limit for the use of the approximate formula describing particle distribution. A rational selectivity coefficient, which is approximately constant over the whole exchange range, only results if a single zeolite crystal consists of one million pseudo-unit-cells or more, or if a sufficiently large number of smaller crystals is considered. On the basis of the statistical particle distribution model, a closed, simple formula for the ion-exchange isotherm is then derived, which is valid for systems involving a variable number of coupled-exchange reactions. Its similarity to the Langmuir isotherm is discussed. The theory on ion-exchange equilibria is used to derive formulae for the change of free-energy, enthalpy, and entropy occurring in coupled ion-exchange reactions. The findings, though applicable to virtually any particle exchanging system with the structural properties described above, are applied to zeolite A, since this material can be treated as a nearly ideal model. The results derived can straightforwardly be used to evaluate experimental data quantitatively, since the common inequivalence of the host sites can be taken into account.

1. Introduction

The domain of host–guest systems based on micro-, meso-, or macroporous materials is a promising field in the development of new functional materials for, for example, imaging techniques, dye lasers of extremely small size, probes in biological systems, (organic) light-emitting diodes, (O)LEDs, and dye-sensitized solar cells.[1–4] The unique features of such host–guest systems depend on factors such as the type of host, the type of guest(s), and the distribution of the guest particles in the host. Hence, a detailed study of the basis of particle distribution within a host helps to advance our understanding of such materials. Zeolites are among the most frequently used host materials. Their spatial constitution is characterized by internal cavities and channels. Depending on the type of zeolite, these differ in number, size, shape, and arrangement. Zeolites are thus able to accommodate various kinds of guests. Classical zeolites are aluminosilicates in which, for each aluminum atom replacing a framework silicon atom, charge compensation with cations is required, some or all of which can be exchanged for other cations. It is the latter feature that is used to explain our reasoning. How can ion exchange in such materials be described on the basis of a simple statistical particle distribution model? We answer this question in several steps that lead to the derivation of an equation for the ion-exchange isotherm. Zeolite A turned out to be an excellent working example. Its cation sites can be treated as if they were equivalent in a first approximation. The theory can be used to evaluate ion-exchange experiments, since the inequivalence of cation sites can be accounted for in the evaluation of experimental results.[5]

The common result of three different derivations of the distribution formula is reported, and we derive formulae for the free-energy, the enthalpy, and the entropy of ion-exchange reactions, based on the particle exchange theory. We intentionally choose a different approach than found in important literature on the statistical-mechanics-based analysis of sorption thermodynamics in zeolites and other crystalline nanoporous solids, because the goals are also different in some aspects. Hence, what we report is not typically statistical-mechanical reasoning, because it is not explicitly based on ensembles and does not involve partition functions. Instead, we initially describe particle distribution by using an exact probabilistic approach, no matter what size the system is. We then consider from what system size on the description, which is valid in the thermodynamic limit, is justified. The same procedure is followed when we describe exchange equilibria. The additional information we gain can be valuable in nanoscience when investigating single particles.

Common research literature in the field of sorption thermodynamics is based on the classical statistical-mechanics approach. Hill was one of the first to present an analysis of sorption thermodynamics, using a lattice model.[6] Ruthven presented a simple theoretical approximate adsorption isotherm for zeolites, which treated the occluded molecules as a van der -

[a] *Dr. M. Meyer, Dr. A. Currao, Prof. Dr. G. Calzaferri*
Department of Chemistry and Biochemistry, University of Bern
Freiestrasse 3, 3012 Bern (Switzerland)
Fax: (+41) 31-631-39-94
E-mail: gion.calzaferri@iac.unibe.ch

Waals gas.[7] He applied this isotherm to the sorption of saturated and unsaturated hydrocarbons and to binary mixtures in type A zeolites.[8,9] In more recent works, adsorption equilibria of various compounds and mixtures in zeolites and other nanoporous materials were simulated using the grand canonical Monte Carlo (GCMC) technique, which allows the simulation of a solid sorbant phase and a liquid or gas phase at equilibrium with a specified chemical potential.[10] Because of the extremely low probability of a successful insertion of longer chain molecules in the host in the exchange step, GCMC simulations for such guests converge poorly. Thus, the configurational-bias MC technique was developed to make the insertion of long-chain molecules in moderately dense liquids possible. Smit showed that this technique can be used in the grand canonical ensemble.[11] Among the many host–guest systems investigated using the GCMC or the configurational-bias GCMC technique are argon, oxygen, and nitrogen in 5A zeolites,[12] xenon, methane, *p*- and *m*-xylene in zeolite Na-Y,[13] alkanes from methane through pentane in AlPO-5,[14] benzene and *p*-xylene in silicalite,[15] linear and branched alkanes in silicalite zeolite,[16] and benzene, cyclohexane, and hexane in AlPO-5.[17]

We do not consider sorbate–sorbate interactions. Sorbate–framework interactions are only considered in a rudimentary way, by letting the enthalpy change occurring in the exchange reactions be a constant, non-zero value. Nevertheless, we can show that in spite of its simplicity, the results can be used for the excellent evaluation of measured ion-exchange isotherms.[5] We initially assume that all cation sites in the host are equivalent. The inequivalence of host sites can be taken into account in a second step. The approach is based on a strictly constant number of particles in the host, and not on a constant chemical potential. In statistical-mechanics language, we make a canonical ensemble approach and not a grand canonical ensemble approach. Analyzing the solid phase in the grand canonical ensemble would have advantages: In typical applications, such as ion exchange, the number of particles in the solid phase is not constant, but is allowed to fluctuate, that is, the solid phase is an open system. It is one of our goals, however, to trace the evolution of our system from microscopic to macroscopic scale, and hence to find out up to what size the system must be described using exact formulae, and from what size on the thermodynamic limit formulae are appropriate. Hence, the investigation requires the closed-system approach we have chosen. In this context, it should be noted that in the field of sorption thermodynamics, not only GCMC simulations have been performed, but also canonical MC simulations.[18]

We first give a structural description of zeolite A. Then, we describe particle distribution in an idealized host, consisting of a fixed number of unit cells, each of them containing a fixed number of equivalent particle sites. In a previous publication, we have presented an approximate approach[19] that has been successfully applied.[20,21] We investigate under what conditions it is justified to use it. We then describe ion-exchange equilibrium via rational selectivity coefficients. Coupled-exchange equilibria have to be considered, since hosts like zeolites have more than one particle site per unit cell. The exact result we find can be simplified if the described system is sufficiently large, and we discuss the required size of the system in order to do so appropriately. We then derive a formula describing ion-exchange isotherms, and compare it to the well-known Langmuir isotherm. Finally, formulae for the thermodynamic quantities of ion-exchange reactions are derived. The results are valid for the description of particle distribution and exchange processes in different crystalline materials. They correspond, in a way, to an "ideal reference system" which can be used as the basis for the introduction of activity coefficients, or for the consideration of nonequivalent particle sites in a host.

2. Zeolite A

Classical zeolites are crystalline aluminosilicates, consisting of an anionic framework and charge-compensating cations. The primary building units are $[SiO_4]$ and $[AlO_4]$ tetrahedra. The framework of the zeolite is assembled by linking these units via oxygen bridges with neighboring tetrahedra sharing one corner. The presence of aluminum leads to a negative charge of the framework, the absolute value of which is equal to the total number of aluminum atoms. This negative charge is compensated by additional cations, which are incorporated in the cavities of the framework.[22] Figure 1 shows the framework as corner-sharing tetrahedra and the resulting three-dimensional channel-structure of zeolite A. The 1:1 ratio between silicon and aluminum in zeolite A is known as Loewenstein's rule, which states that no two aluminum tetrahedra can be neighbors in the framework.[23,24] Two kinds of structural subunits are formed. The smaller of these units consists of 24 tetrahedra and is commonly denoted as β-cage, sodalite cavity, or pseudo-unit-cell. It is shown on the right side, including shaded 4- and 6-membered rings into which its surface can be divided. The larger structural subunit formally consists of 48 tetrahedra. The surface of this so-called α-cage is seen to be split-up into 4-, 6-, and 8-membered rings. Zeolite A can be imagined as being built up by octahedrally assembled α- or β-cages. The α-cages are joined directly, every two α-cages sharing one 8-ring. The β-cages are joined at the 4-rings via four bridging oxygen atoms. Figure 1c shows an assembly of eight α-cages forming a sodalite cavity (β-cage) in their common center. Also shown are the cubes that bridge the β-cage with its neighbors. The assembly shown in Figure 1c is one crystallographic unit cell of zeolite A. One α-cage alone cannot form a unit cell, since corresponding positions in neighboring α-cages are alternately occupied by silicon and aluminum atoms. Therefore, two α-cages are needed along all three crystallographic axes to form one repeating unit. Taking into account the intracrystalline water, which fills the channels and cavities of zeolites under ambient conditions, the formula of one pseudo-unit-cell is $M^+_{12}[(AlO_2)^-_{12}\ (SiO_2)_{12}]{\cdot}xH_2O$. The number x of intracrystalline water molecules per pseudo-unit-cell depends on the cation M^+. In the case of sodium, x equals 27, in the case of potassium and silver, x equals 24. More detailed structural information on zeolite A in particular, and on zeolites in general, can be found in refs. [25,26]. Zeolite A was first syn-

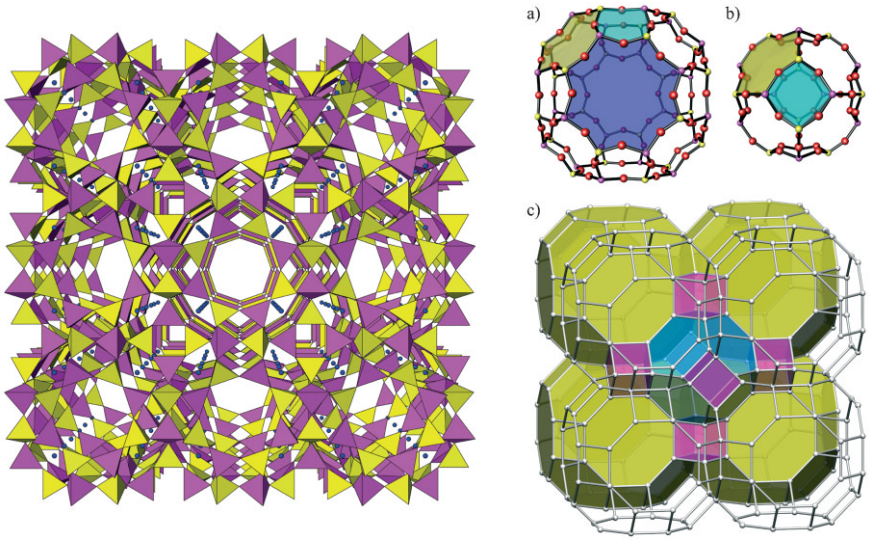

Figure 1. Structure and framework of zeolite A. Left: The $[AlO_4]$ tetrahedra are magenta shaded and the $[SiO_4]$ tetrahedra yellow. The small blue globules represent the charge-compensating, monovalent cations. Right: a) α-cage and b) β-cage. The globules represent silicon (yellow), aluminum (magenta), and oxygen (red) atoms. The oxygen atoms which form bridges between neighboring β-cages are not shown. The shadings show the constituent rings of the cages. c) Eight α-cages, forming the unit cell of zeolite A. Note that the oxygen atoms are omitted here. The four rear α-cages are yellow shaded. The blue-shaded central region shows a β-cage, which is created through the assembling of α-cages. The cubes connecting adjacent β-cages are magenta shaded.

thesized by Breck and co-workers[27,28] and some recent developments in its preparation have been reported in ref. [29].

3. Particle Distribution

We assume a system of N_{uc} unit cells with n_{box} equivalent sites per unit cell, each site having a capacity of one particle. A number of i particles are then distributed arbitrarily among the sites, every site having the same probability to receive a particle, resulting in a distribution of the particles among the $N_{uc}{\cdot}n_{box}$ sites. This abstract model can be related for example, to the ion-exchange system zeolite A, where each of the N_{uc} pseudo-unit-cells can incorporate $n_{box}=12$ monovalent, monoatomic charge-compensating cations. These ions can be exchanged for other cations, for example, for silver ions, resulting in a distribution of the two ionic species among the $N_{uc}{\cdot}n_{box}$ sites. The positions of the cations in dehydrated zeolite Na–A have been precisely determined.[30] Although it has been known for a long time that the cation positions are not perfectly equivalent,[31] their equivalence is presumed as a first approximation. The inequivalence of the sites can later be simply taken into account by the segmental analysis of the isotherms.[5] The resulting particle distribution can be characterized by $\mu(r,i)$, the expected value of the number of unit cells containing r particles, with r ranging from 0 to n_{box}. Obviously, Equations (1) and (2) must hold.

$$0 \le \mu(r,i) \le N_{uc} \tag{1}$$

$$\sum_{r=0}^{n_{box}} \mu(r,i) = N_{uc} \tag{2}$$

The formula for $\mu(r,i)$ has been derived using a hypergeometric, a probabilistic, and a recursive approach, all leading to the result expressed in Equation (3):[32]

$$\mu(r,i) = N_{uc}\frac{\binom{n_{box}}{r}\binom{N_{uc}n_{box}-n_{box}}{i-r}}{\binom{N_{uc}n_{box}}{i}} \tag{3}$$

As an example to explain this result, we assume we have $N_{uc}=3$ unit cells, each one of them containing $n_{box}=7$ sites, which are filled with $i=10$ particles. Figure 2 shows an arbitrarily chosen distribution.

There are 352716 possible ways to distribute the ten particles among the three unit cells. There

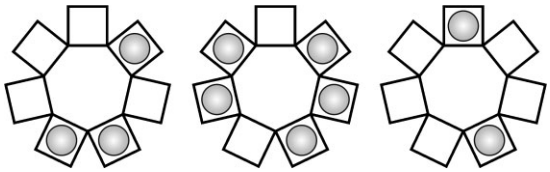

Figure 2. Arbitrary distribution of $i=10$ particles among $N_{uc}=3$ unit cells, each cell containing $n_{box}=7$ sites. The case shown is an example of a distribution of type (5,3,2).

are, for example, 124803 distributions with one or two unit cells containing five particles. These distributions originate from 1323 cases of type (5,5,0), 30870 cases of type (5,4,1), and 92610 cases of type (5,3,2). The following expected value of the number of unit cells containing five particles results, see Equation (4):

$$\begin{aligned}\mu(5,10) = {} & p((7,3,0))\cdot 0 + p((7,2,1))\cdot 0 + p((6,4,0))\cdot 0 \\ & + p((6,3,1))\cdot 0 + p((6,2,2))\cdot 0 + p((5,5,0))\cdot 2 \\ & + p((5,4,1))\cdot 1 + p((5,3,2))\cdot 1 + p((4,4,2))\cdot 0 \\ & + p((4,3,3))\cdot 0 \\ = {} & \frac{231}{646}\end{aligned} \tag{4}$$

Using Equation (3), we get Equation (5):

$$\mu(5,10) = 3\frac{\binom{7}{5}\binom{14}{5}}{\binom{21}{10}} = \frac{231}{646} \tag{5}$$

The hypergeometric distribution is approximated by the binomial distribution [Eq. (6)]:

$$P_i(r) = \binom{i}{r}\left(\frac{1}{N_{uc}}\right)^r\left(1-\frac{1}{N_{uc}}\right)^{i-r} \quad (6)$$

which is valid if $i/N_{uc}n_{box} < 0.1$ and $N_{uc}n_{box} \geq 60$. The first restriction prevents us from using it, since we are not only interested in filling degrees up to 10%. In ref. [19], we have therefore used another way to approximately describe particle distribution. The expected value of the number of unit cells containing r particles after adding the ith particle is given by Equation (7):

$$N(r,i) = N_{uc}\binom{n_{box}}{r}\left(\frac{i}{N_{uc}n_{box}}\right)^r\left(\frac{N_{uc}n_{box}-i}{N_{uc}n_{box}}\right)^{n_{box}-r} \quad (7)$$

The following example shows that Equation (7), subsequently denoted as the binomial distribution, is not a precise description of the particle distribution model: We assume a system consisting of $N_{uc}=4$ unit cells, each cell containing $n_{box}=10$ sites. The system is filled with $i=5$ particles. The expected value of the number of unit cells containing $r=7$ particles obviously must be zero. Equation (8) confirms this:

$$\mu(7,5) = 4\frac{\binom{10}{7}\binom{30}{-2}}{\binom{40}{5}} = 4\frac{120\cdot 0}{658\,008} = 0 \quad (8)$$

Here, we have used the well-known Gamma function [Eq. (9)]:

$$\binom{30}{-2} = \binom{30}{32} = \lim_{t\to 0}\frac{\Gamma(31+t)}{\Gamma(33)\Gamma(-1+t)} = 0 \quad (9)$$

However, the binomial distribution returns a non-zero value [Eq. (10)]:

$$N(7,5) = 4\binom{10}{7}\left(\frac{5}{40}\right)^7\left(\frac{35}{40}\right)^3 = 1.53\underline{3}\times 10^{-4} \quad (10)$$

This non-zero value originates from the fact that Equation (7) is non-zero from $r=0$ to $r=n_{box}$, no matter whether r is larger or smaller than i. Also, the expected value of the number of unit cells containing no particle when the first particle has been distributed must in this system be equal to exactly three. The results of Equations (3) and (7) are given by Equations (11) and (12):

$$\mu(0,1) = 4\frac{1\cdot 30}{40} = 3 \quad (11)$$

$$N(0,1) = 4\cdot 1\left(\frac{1}{40}\right)^0\left(\frac{39}{40}\right)^{10} = 3.10\underline{5} \quad (12)$$

While the binomial distribution does not precisely describe particle distribution, the decisive question is, rather, whether it is an appropriate approximation to describe particle distributions in the systems we are interested in. We have shown that the specific form of the binomial distribution allows the derivation of a simple recursive formula for the rational selectivity coefficients as used, for example, to describe monovalent ion-exchange equilibria in zeolites.[19] Hence, the usefulness of the binomial approach is obvious. It is justifiable if we can show that, under conditions that are typically fulfilled in a realistic situation, $\mu(r,i)$ and $N(r,i)$ are asymptotically equal. We have shown that the following limit, Equation (13) holds:[32]

$$\lim_{\substack{N_{uc}n_{box}\to\infty\\ i\to\infty}}\frac{\mu(r,i)}{N(r,i)} = 1 \quad (13)$$

The limit is reached if the number of distributed particles is large, thus fulfilling $i\to\infty$, but significantly smaller than the number of sites, thus fulfilling $N_{uc}n_{box}-i\to\infty$. Consequently, we can say that the binomial approach is a good approach for moderate filling degrees in a large system. However, if the system is nearly empty or nearly full, the quotient of the two formulae significantly deviates from 1. We visualize $N(r,i)/\mu(r,i)$ for $n_{box}=10$ and $r=7$ in Figure 3.

Figure 3a shows the situation for a small number of unit cells. We see that indeed $N(r,i)/\mu(r,i)$ significantly deviates from 1 for small values of i and for small values of $N_{uc}n_{box}-i$. Since

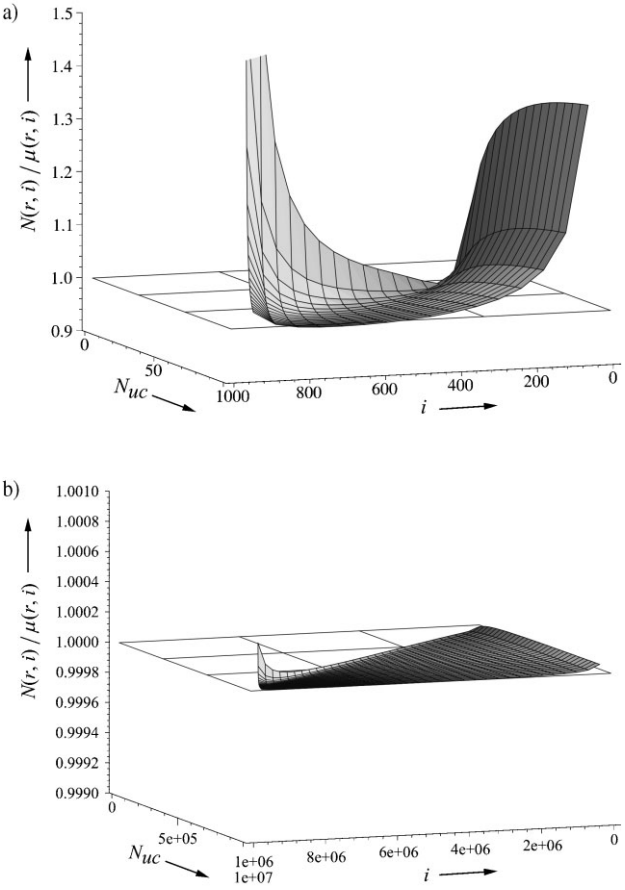

Figure 3. Fraction of the distribution formulae for the binomial and for the exact approach. a) $N(7,i)/\mu(7,i)$ for $n_{box}=10$; $0\leq N_{uc}\leq 100$, $0\leq i\leq 1000$. b) $N(7,i)/\mu(7,i)$ for $n_{box}=10$; $0\leq N_{uc}\leq 1\,000\,000$, $0\leq i\leq 10\,000\,000$.

Table 1. Comparison of $N(7,i)/\mu(7,i)$ and $N(7,i)-\mu(7,i)$ for $n_{box}=10$ and $N_{uc}=200$.

	$N(7,i)$	$\mu(7,i)$	$N(7,i)/\mu(7,i)$	$N(7,i)-\mu(7,i)$
$i=7$	$0.15280\cdot10^{-12}$	$0.95\cdot10^{-15}$	160.00	$0.15184\cdot10^{-12}$
$i=1000$	23.4375	23.4021	1.0015	0.0354
$i=1997$	$8.01533\cdot10^{-5}$	$1.80270\cdot10^{-5}$	4.44628	0.00006

the system is small, these border effects play a larger role, because the values of i which yield a significant deviation make up a relatively large percentage of all possible values of i. Figure 3b visualizes the situation for a larger system. Here, the border effects become prominent only at the outermost margins. Since, in systems with a million unit cells or more, significant border effects appear only in a negligibly narrow region, we conclude that the use of the binomial approximation is highly justified in large systems. Typical zeolite A crystals are cubes with an edge length of about 1 μm.[29] They contain about 537 million pseudo-unit-cells per crystal, which lies high above the situation illustrated in Figure 3b. Hence, the conditions for the use of the binomial approximation are fulfilled. According to the above considerations, restrictions to the usability of the binomial approximation for the description of large systems have to be made only at extremely low and high-filling degrees. In fact, not even these restrictions need to be upheld: While $N(r,i)/\mu(r,i)$ becomes large for small values of i and for small values of $N_{uc}n_{box}-i$, $N(r,i)-\mu(r,i)$ becomes negligibly small in these regions. The limits in Equations (14) and (15) have been derived in ref. [32]. A numeric example is given in Table 1.

$$\lim_{i\to 0} N(r,i)-\mu(r,i)=0 \tag{14}$$

$$\lim_{i\to N_{uc}n_{box}} N(r,i)-\mu(r,i)=0 \tag{15}$$

We conclude that the binomial approximation can be used to describe particle distribution appropriately, in reasonably large systems, without any further restrictions. By reaching the thermodynamic limit by enlargement of the system, the binomial description becomes precise. In the case of zeolite A, a hypothetical cubic crystal with an edge length of 12 nm, and hence containing about 1000 pseudo-unit-cells, fixes a lower limit for the use of the binomial approximation, thus showing that this approximation is even applicable to single nanoparticles. This is visualized in Figure 4 by a plot of the particle distribution functions $\overline{N}(r,p)$ and $\overline{\mu}(r,p)$, expressing the dependence of the normalized expected values of the number of unit cells containing r particles on the filling degree p of the system [Eq. (16)]:

$$\overline{N}(r,p)=\frac{N(r,N_{uc}n_{box}p)}{N_{uc}} \quad \overline{\mu}(r,p)=\frac{\mu(r,N_{uc}n_{box}p)}{N_{uc}} \quad p\in[0,1] \tag{16}$$

The red arrays of curves correspond to $\overline{N}(r,p)$, while the blue ones correspond to $\overline{\mu}(r,p)$. Each curve of an array corresponds to the value of r denoted next to it. $n_{box}=10$ in all cases. $N_{uc}=3$, 10, and 1000 in Figures 4a, b, and c, respectively, thus representing single nanocrystals of different size.

4. Exchange Equilibria

4.1. Rational Selectivity Coefficients

Filling in i particles of species A in an empty system, consisting of $N_{uc}n_{box}$ sites, can be understood as replacing i empty sites with filled sites. A physically different, but mathematically equivalent, situation occurs if the sites are initially not empty but filled with particles of another species, B, i of which are

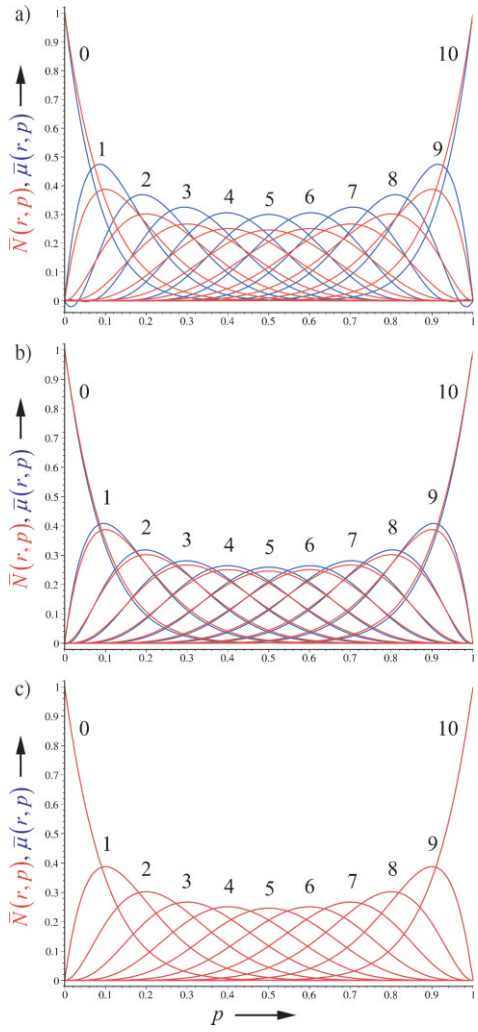

Figure 4. Dependence of the particle distribution functions $\overline{N}(r,p)$ (red) and $\overline{\mu}(r,p)$ (blue), expressing the normalized expected values of the number of unit cells containing r particles, on the filling degree p of the system, with p ranging from 0 to 1, for single nanocrystals of different size. Each curve corresponds to the value of r next to it. $n_{box}=10$. a) $N_{uc}=3$, b) $N_{uc}=10$, c) $N_{uc}=1000$. The negative values of $\overline{\mu}(r,p)$, visible in (a) are due to p continuously running from 0 to 1. However, $\mu(r,i)$ and hence $\overline{\mu}(r,p)$ only have a physical meaning for non-negative integer values of i, that is, if $N_{uc}n_{box}p$ is integral.

then exchanged for particles of species A. This second situation represents ion-exchange phenomena typical for zeolites. When such an exchange is performed, the initial state of all unit cells (pseudo-unit-cells in the case of zeolite A) Z is $ZB_{n_{box}}$, which means that each unit cell is filled with the maximum number of n_{box} particles B. The equilibria shown in Equation (17) are then reached:[19]

$$\begin{array}{rcll} ZB_{n_{box}} + A & \rightleftharpoons & ZAB_{n_{box}-1} + B & K_1 \\ ZAB_{n_{box}-1} + A & \rightleftharpoons & ZA_2B_{n_{box}-2} + B & K_2 \\ ZA_2B_{n_{box}-2} + A & \rightleftharpoons & ZA_3B_{n_{box}-3} + B & K_3 \\ \vdots & & \vdots & \vdots \\ ZA_{n_{box}-1}B + A & \rightleftharpoons & ZA_{n_{box}} + B & K_{n_{box}} \end{array} \quad (17)$$

The equilibria can be described using rational selectivity coefficients K_r [Eq. (18)]:

$$K_r = \frac{[ZA_rB_{n_{box}-r}][B]}{[ZA_{r-1}B_{n_{box}-(r-1)}][A]} \quad r = 1,2,\ldots,n_{box} \quad (18)$$

Forming the ratio between K_r and K_{r+1} yields Equation (19):

$$\frac{K_r}{K_r+1} = \frac{[ZA_rB_{n_{box}-r}]^2}{[ZA_{r-1}B_{n_{box}-(r-1)}][ZA_{r+1}B_{n_{box}-(r+1)}]} \quad r = 1,2,\ldots,n_{box}-1 \quad (19)$$

Equation (19) describes the following equilibria that correspond to the internal occupation equilibrium [Eq. (20)]:

$$\begin{array}{rcl} ZB_{n_{box}} + ZA_2B_{n_{box}-2} & \rightleftharpoons & 2ZAB_{n_{box}-1} \\ ZAB_{n_{box}-1} + ZA_3B_{n_{box}-3} & \rightleftharpoons & 2ZA_2B_{n_{box}-2} \\ ZA_2B_{n_{box}-2} + ZA_4B_{n_{box}-4} & \rightleftharpoons & 2ZA_3B_{n_{box}-3} \\ \vdots & & \vdots \\ ZA_{n_{box}-2}B_2 + ZA_{n_{box}} & \rightleftharpoons & 2ZA_{n_{box}-1}B \end{array} \quad (20)$$

Equation (20) makes it obvious that the equilibrium concentrations of all species in Equation (19) can be replaced by the expected values of the corresponding number of unit cells in the system, since the volume of the system is constant, the ion-exchange and the particle distribution model are equivalent and the equilibria in Equation (20) are established statistically [Eq. (21)]:

$$\frac{K_r}{K_{r+1}} = \frac{\mu(r,i)^2}{\mu(r-1,i)\mu(r+1,i)} \quad \begin{array}{l} r = 1,2,\ldots,n_{box}-1 \\ r < i < N_{uc}n_{box} - n_{box} + r \end{array} \quad (21)$$

where i is the number of particles incorporated in the host system. In the case of the system in Equation (17) this number is only determined after the system is equilibrated. The restrictions on i arise from the need of each equilibrium shown in Equation (17)—or (20)—to exist.

Using Equation (3), Equation (21) can be rewritten in a recursive form [Eq. (22)]:

$$K_{r+1} = K_r \underbrace{\left(\frac{r+1}{r}\frac{i-r+1}{i-r}\frac{n_{box}-r+1}{n_{box}-r}\frac{N_{uc}n_{box}-n_{box}-i+r+1}{N_{uc}n_{box}-n_{box}-i+r}\right)^{-1}}_{c_r}$$
$$r = 1,2,\ldots,n_{box}-1 \quad (22)$$
$$r < i < N_{uc}n_{box} - n_{box} + r$$

It is easily seen that the second factor in the bracket approaches 1 when $i \gg r$ and that the fourth factor approaches 1 when $i \ll N_{uc}n_{box} - n_{box} + r$. If these conditions are fulfilled, Equation (22) can be approximated by Equation (23):

$$K_{r+1} \approx K_r\left(\frac{r+1}{r}\frac{n_{box}-r+1}{n_{box}-r}\right)^{-1} \quad \begin{array}{l} r = 1,2,\ldots,n_{box}-1 \\ r \ll i \ll N_{uc}n_{box} - n_{box} + r \end{array} \quad (23)$$

Hence, the larger a system is, the better Equation (23) is fulfilled, because, with increasing system size, the fraction of the values of i which well-fulfill $r \ll i \ll N_{uc}n_{box} - n_{box} + r$ increases, too. (Note that the system grows when N_{uc} grows, whereas n_{box} is a system constant.) Consequently, Equation (23) precisely describes the recursive dependence between the selectivity coefficients describing the equilibria shown in Equation (17) in the limiting case of an infinitely large system. In the case of a zeolite A crystal consisting of one million pseudo-unit-cells, for example, ($N_{uc} = 10^6$, $n_{box} = 12$), Equation (23) is suitable for particle numbers ranging from about $\frac{1}{1000}N_{uc}n_{box} = 12\,000$ up to about $\frac{999}{1000}N_{uc}n_{box} = 11\,988\,000$. The same formula results when using the binomial distribution, Equation (7).[19] The fact that both approaches lead to the same formula nicely supports our findings, that is, that the two distributions converge when the system grows. Explicit formulae for K_r can be formulated. The formula corresponding to the precise recursive definition, Equation (22), is Equation (24):

$$K_r = \frac{K_1}{r}\frac{i-r+1}{i}\frac{n_{box}-r+1}{n_{box}}\frac{N_{uc}n_{box}-n_{box}-i+1}{N_{uc}n_{box}-n_{box}-i+r}$$
$$r = 1,2,\ldots,n_{box} \quad (24)$$
$$r \le i \le N_{uc}n_{box} - n_{box}$$

The compatibility of the explicit with the recursive formula can easily be verified by forming the fraction of K_{r+1} over K_r using Equation (24) [Eq. (25)]:

$$\frac{K_{r+1}}{K_r} = \frac{r(i-r)(n_{box}-r)(N_{uc}n_{box}-n_{box}-i+r)}{(r+1)(i-r+1)(n_{box}-r+1)(N_{uc}n_{box}-n_{box}-i+r+1)} = c_r \quad (25)$$

$$r = 1,2,\ldots,n_{box}-1$$
$$r < i < N_{uc}n_{box} - n_{box} + r$$

Note that Equation (24) yields $K_r = K_1$ if $r = 1$, which is joyful.

The condition $r \ll i \ll N_{uc}n_{box} - n_{box}$ allows Equation (24) to be simplified—just as Equation (22) was simplified—giving Equation (26):

$$K_r \approx K_1 \frac{n_{box} - r + 1}{n_{box} r} \quad \begin{matrix} r = 1, 2, \cdots, n_{box} \\ r \ll i \ll N_{uc} n_{box} - n_{box} \end{matrix} \tag{26}$$

This approximate formula for the individual rational selectivity coefficients describing the equilibria shown in Equation (17) becomes exact if the system becomes infinitely large. Since $r \ll i \ll N_{uc}n_{box} - n_{box}$ is typically fulfilled in, for example, a zeolite crystal, Equation (26) is adequate for describing the selectivity coefficients of ion-exchange equilibria in idealized zeolites with equivalent particle sites. We now consider the equilibrium for the complete exchange of all ions [Eq. (27)]:

$$ZB_{n_{box}} + n_{box}A \rightleftharpoons ZA_{n_{box}} + n_{box}B \quad K_{tot} \tag{27}$$

The corresponding rational selectivity coefficient is easily seen to be equal to the product of the rational selectivity coefficients of all equilibria involved [Eq. (28)]:

$$K_{tot} = \frac{[ZA_{n_{box}}][B]^{n_{box}}}{[ZB_{n_{box}}][A]^{n_{box}}} = \prod_{r=1}^{n_{box}} K_r \tag{28}$$

Substitution of all K_r, using Equation (24), yields Equation (29):

$$K_{tot} = \left(\frac{K_1}{n_{box}}\right)^{n_{box}} \left(\frac{N_{uc}n_{box} - n_{box} + 1 - i}{i}\right)^{n_{box}-1} \prod_{\lambda=1}^{n_{box}-1} \frac{i - \lambda}{N_{uc}n_{box} + 1 - i - \lambda} \tag{29}$$

$$n_{box} \leq i \leq N_{uc}n_{box} - n_{box}$$

Assuming the same conditions as above, we can again greatly simplify and find Equation (30):

$$K_{tot} \approx \left(\frac{K_1}{n_{box}}\right)^{n_{box}} \quad n_{box} \ll i \ll N_{uc}n_{box} - n_{box} \tag{30}$$

K_1 as well as all other coefficients K_r are not categorically constant for small systems, but depend on the number of particles i. This is visualized in Figure 5a, where we show K_2 through K_{12} as a function of i for a system consisting of only ten unit cells, each of them containing twelve particle sites. In order to be able to use Equation (24), we have chosen the constant value 1 for K_1. The fact that the deviation from constancy increases with decreasing r indicates that K_1 would actually show the strongest deviation from constancy. At first glance, the simultaneous decay of all K_r at $i = N_{uc}n_{box} - n_{box}$ is puzzling. However, if $i = N_{uc}n_{box} - n_{box} + 1$ particles were present in the system, this would mean that, in the equilibration process, each unit cell would have exchanged at least one particle. Consequently, K_1 (and hence, due to Equation (26), all K_r) would have to be infinitely large. This contradicts the precondition $K_1 = 1$. As a result, since K_1 must be finite, the system can only exist up to $i = N_{uc}n_{box} - n_{box}$, *and this value is thus the ultimate limit for the coefficients* K_r *describing the equilibrated system, to have a sensible value. Figure 5b shows that when the system becomes large, the coefficients* K_r *approach constancy, provided that* K_1 *is constant.*

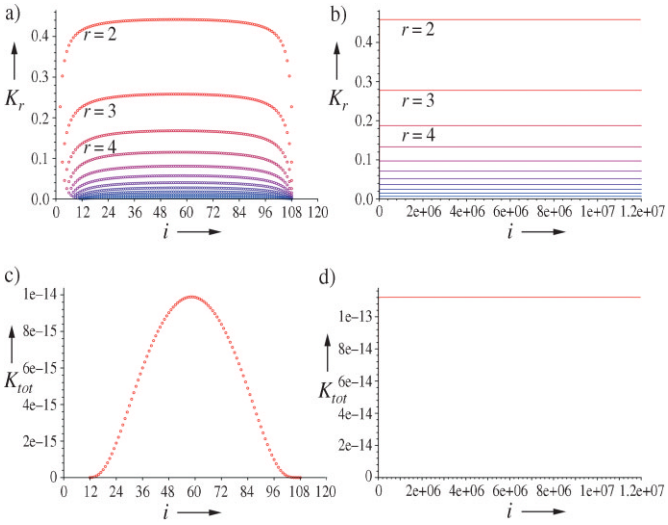

Figure 5. Investigation of the constancy of K_r and K_{tot} for a small crystal and for a large system. a,b) K_2 (red) through K_{12} (blue), using Equation (24) with $K_1 = 1$: a) for a very small system ($N_{uc} = 10$, $n_{box} = 12$) and b) for a large system ($N_{uc} = 10^6$, $n_{box} = 12$) versus the number of particles i. c,d) K_{tot}, using Equation (29) with $K_1 = 1$: c) for a very small system ($N_{uc} = 10$, $n_{box} = 12$) and d) for a large system ($N_{uc} = 10^6$, $n_{box} = 12$) versus the number of particles i.

While not directly provable, it is obvious that K_1 *undergoes the very same development with increasing system size. We conclude that, in sufficiently large systems, all selectivity coefficients* K_r *are constant, their value being given by Equation (26). In Figure 5c,* K_{tot}, *calculated using Equation (29) with* $K_1 = 1$, *is plotted versus* i *for* $N_{uc} = 10$ *and* $n_{box} = 12$, *while Figure 5d visualizes* K_{tot} *for* $N_{uc} = 10^6$ *and* $n_{box} = 12$.

K_{tot} strongly depends on the number of exchanged particles in small systems. This is a direct consequence of the same property of the individual K_r, since K_{tot} is their product. For the same reason, K_{tot} must approach constancy when the system becomes large. This is observed in Figure 5d, and corresponds to the familiar constancy of rational selectivity coefficients in macroscopic systems. In fact, these are still much larger than the system of Figure 5d. We conclude that rational selectivity coefficients describing ion-exchange equilibria approach constancy when the size of the system approaches the thermodynamic limit. The transition from Equations (22), (24), and (29) to Equations (23), (26), and (30), respectively, therefore corresponds to the transition to the thermodynamic limit. When we derive formulae describing sorption thermodynamics in Sections 4.2 and 4.3, we therefore base all derivations on Equations (23), (26), and (30).

Before closing this section, we mention three additional aspects: First we consider the rates of the selectivity coefficients K_r of the equilibria shown in Equation (17). Equation (22) shows that the K_r form a sequence, the members of which are linked by the factors c_r. These factors all lie between 0 and 1, resulting in a monotonic decrease in the selectivity coefficients with increasing r. The algebraic form of the factors c_r, given in Equation (22), immediately shows that this is generally true. Secondly, the decrease in factors c_r are practically symmetric with respect to $r = n_{box}/2$. This is a consequence of the approximate

equality given in Equation (31):

$$c_r \approx c_{n_{box}-r} \tag{31}$$

that is exactly fulfilled in the limiting case of Equation (23). Thirdly, Figure 6, a plot of $\ln(K_r/K_1)$ as a function of r, shows that the rational selectivity coefficients decrease faster for low and for high values of r.

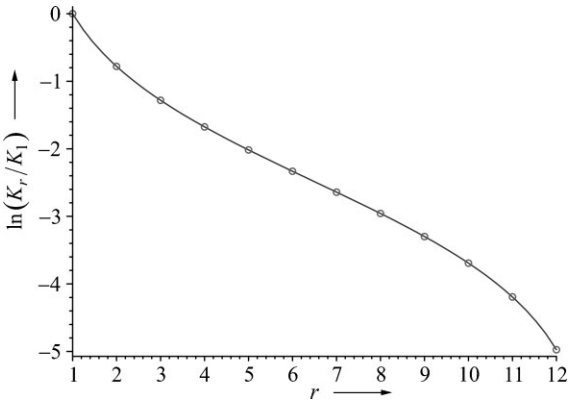

Figure 6. Plot of $\ln(K_r/K_1)$, using Equation (24), for $r=1,2,3,\ldots12$ for the system $N_{uc}=1000$, $n_{box}=12$ at an exchange degree of 50% ($i=6000$), ○. The curve visualizes the function $\ln(K(r)/K(1))$, generated from Equation (24), in the interval [1,12] for the same system.

4.2. Exchange Isotherms

Exchange isotherms are a common way to depict ion-exchange reactions. These are plots of the equivalent fraction of the exchanging species in the host versus its equivalent fraction in the solution, measured under equilibrium conditions and at constant temperature. Given an ionic species, its equivalent amount of substance, also called the number of equivalents, is the amount of substance, weighted by the charge of one ion. Consequently, the equivalent fraction of ionic species A in an environment is the ratio of the number of equivalents of A in the environment and the total number of equivalents of all ionic species under consideration in the environment. Thus, in the special case of an ion-exchange reaction, with ions of species A exchanging ions of species B in a host H, the equivalent fraction of A in the host, H_A, is given by Equation (32):

$$H_A = \frac{\text{number of equivalents of A in the host}}{\text{total number of equivalents of A and B in the host}} \tag{32}$$

If a and b are the charges of the ions A and B, respectively, then the equivalent fraction of A in the solution, S_A, is given by Equation (33):

$$S_A = \frac{a[A]}{a[A]+b[B]} \tag{33}$$

The concentration in molarities of any of the species $ZA_rB_{n_{box}-r}(r=1,2,\ldots,n_{box})$ occurring in the reactions in Equation (17) can be described using Equation (34):[32]

$$\left[ZA_rB_{n_{box}-r}\right] = \frac{\frac{[A]^r}{[B]^r}\prod_{j=1}^{r}K_j}{\sum_{i=0}^{n_{box}}\left[\frac{[A]^i}{[B]^i}\prod_{j=1}^{i}K_j\right]}[Z]_{tot} \quad r=1,2,\ldots,n_{box} \tag{34}$$

The total concentration of bound species A is obviously described by Equation (35):

$$[A_{bound}]_{tot} = \sum_{\rho=1}^{n_{box}} \rho\left[ZA_\rho B_{n_{box}-\rho}\right] \tag{35}$$

Assuming monovalent cations A and B, H_A and S_A can then be formulated by Equations (36) and (37):

$$H_A = \frac{[A_{bound}]_{tot}}{n_{box}[Z]_{tot}} \tag{36}$$

$$S_A = \frac{[A]}{[A]+[B]} \tag{37}$$

H_A can be transformed into Equation (38) by using Equations (35), (34), and (26):

$$H_A = \frac{[A]K_1}{[A]K_1 + n_{box}[B]} \tag{38}$$

H_A can also be expressed as a function of S_A instead of [A] and [B], by using Equation (37) [Eq. (39)]:

$$H_A = \frac{K_1 S_A}{(K_1 - n_{box})S_A + n_{box}} \tag{39}$$

Hence, we have handy formulae describing the equivalent fraction of the exchanging ion in the host in an ion-exchange reaction. H_A in the form of Equation (38) is formally similar to the Langmuir isotherm describing the adsorption of free gas molecules on a solid surface [Eq. (40)]:[33]

$$\theta = \frac{pK}{pK+1} \tag{40}$$

where θ is the fractional coverage of the surface, corresponding to the equivalent fraction of exchanged particles, H_A; p is the pressure of the gas, corresponding to the concentration of free A in the solution, [A]; K is the equilibrium constant describing the equilibrium between adsorption and desorption of the gas molecules, corresponding to the equilibrium constant K_1 of the first equilibrium of Equation (17). The Langmuir isotherm is based on three assumptions: 1) Adsorption cannot proceed beyond monolayer coverage. 2) All sites of an adsorbing surface are equivalent, and the surface is uniform. 3) The ability of a molecule to adsorb at a given site is independent of the occupation of neighboring sites. In the particle distribution model, each of these assumptions has a counterpart, thus showing that the formal similarity of Equations (38) and (40) is not surprising: The fact that each site in the host can only be

occupied by one particle at the same time corresponds to (1). The equivalence of all sites and their independence, corresponding to (2) and (3), are key preconditions of the particle distribution model that have been presumed in Section 3. The differences between Equations (38) and (40) result from the coupling of more than one exchange reaction in our system, and from the fact that we have exchange and not only adsorption: Each "adsorbed" particle "desorbs" one particle. If one takes this into account, the derivation of the Langmuir isotherm yields the special case of Equation (38) for $n_{box}=1$. Hence, the equivalence of ion-exchange isotherms and Langmuir isotherms, already reported some years ago,[34] can be derived on the basis of a statistical particle distribution model. In Figure 7, we plot H_A as a function of S_A, according to Equation (39), using various values for K_1 and n_{box}, thus generating typical ion-exchange isotherms.

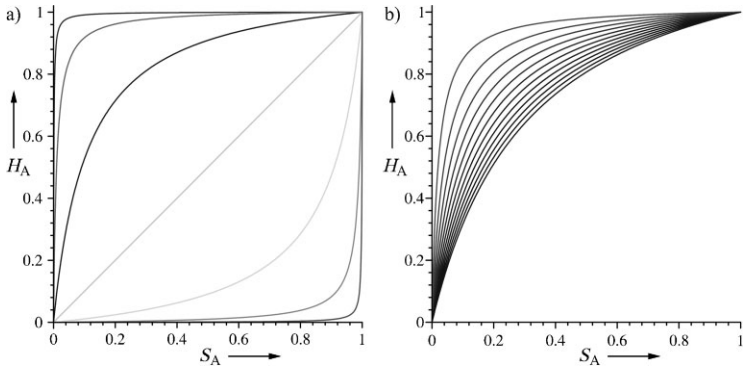

Figure 7. Plots of H_A as a function of S_A according to Equation (39). a) $n_{box}=10$, $K_1=10^{-2}$, 10^{-1},…, 10^4. b) $K_1=50$, $n_{box}=1,2,3,\ldots12$.

4.3. The Thermodynamic Quantities ΔH, ΔS, and ΔG

We consider the thermodynamic quantities ΔH, ΔS, and ΔG of the individual exchange reactions in Equation (17), and of the coupled system of these reactions, all quantities referring to one mole of pseudo-unit-cells. We assume that activities do not have to be considered (condition 1), and that there is an equal change of enthalpy in all n_{box} individual exchange reactions (condition 2). Both conditions define an ideal reference system, the latter because it implies that all cation sites are equivalent and independent of each other [Eqs. (41) and (42)]:

$$\Delta G_r = -RT\ln K_r \tag{41}$$

$$\Delta H - T\Delta S_r = -RT\ln K_r \tag{42}$$

where ΔH is the common enthalpy change any of the n_{box} reactions involved, while ΔS_r and ΔG_r denote the specific change of entropy and free-energy resulting from the rth reaction, respectively. We now calculate ΔH_{tot}, ΔS_{tot}, and ΔG_{tot} for the coupled system of the n_{box} reactions in Equation (17). In a first approach, we use the additional third condition that ΔH is equal to zero [Eqs. (43) and (44)]:

$$\Delta H_{tot} = n_{box}\Delta H = 0\ \mathrm{kJ\,mol^{-1}} \tag{43}$$

$$\Delta S_r = R\ln K_r \tag{44}$$

The total change of entropy is the sum of the n_{box} individual changes. Using Equation (28), we find Equations (45) and (46):

$$\Delta S_{tot} = \sum_{r=1}^{n_{box}} \Delta S_r = R\ln\left(\prod_{r=1}^{n_{box}} K_r\right) = R\ln K_{tot} \tag{45}$$

$$\Delta G_{tot} = \Delta H_{tot} - T\Delta S_{tot} = -RT\ln K_{tot} \tag{46}$$

Since we assume that there is no enthalpy change, the equilibrium constants are purely determined by the entropy changes. This means that the exchanging, as well as the exchanged, species have the same selectivity for the host and for the environment of the host. Hence, the exchange of two specific particles happens with a probability of 50%. The two species can be imagined as globules filling an array of equal boxes, with one globule per box. One subarray corresponds to the host, the complementary subarray to the environment of the host. The globules, differing in color but otherwise identical, are then arbitrarily exchanged between the boxes. After equilibrium has been established, they are uniformly distributed among the boxes. Figure 8 visualizes the situations before (top) and after (middle) equilibration. We now derive formulae for ΔH_{tot}, ΔS_{tot}, and ΔG_{tot} without using condition 3. Here, the selectivity coefficients are not only determined by the entropy change, but also by the enthalpy change. This means that the exchanging and the exchanged species have a different selectivity for the sites in the host, resulting in a probability different from 50% for the exchange of two specific particles. One can also say that the two species are not equivalent if the third condition is not fulfilled. If the exchanging species has a higher selectivity for the host sites than the species being exchanged, this results in a final state as shown in the bottom part of Figure 8.

A non-zero value of ΔH influences the individual selectivity coefficients K_r of the equilibria in Equation (17) by yielding a higher or lower average number of exchanged particles in the host after equilibration. However, the distribution of the particles within the host is still only governed entropically, because the exchange reactions in Equation (20) involve no enthalpy change. This is so because all particle sites are assumed to be equivalent. In turn, the entropic regime is an indispensable precondition for the use of the particle distribution formula in Equation (21), and only this enables the derivation of the simple formulae of Section 4.1.

We see that the entropy change of the rth reaction of Equation (17) is approximately a linear function of $\ln(K_r/K_1)$, if we write, using Equation (42) [Eq. (47)]:

$$\Delta S_r = \frac{\Delta H}{T} + R\ln K_r = R\ln\frac{K_r}{K_1} + \underbrace{R\ln K_1 + \frac{\Delta H}{T}}_{\text{const. for const. } T} \tag{47}$$

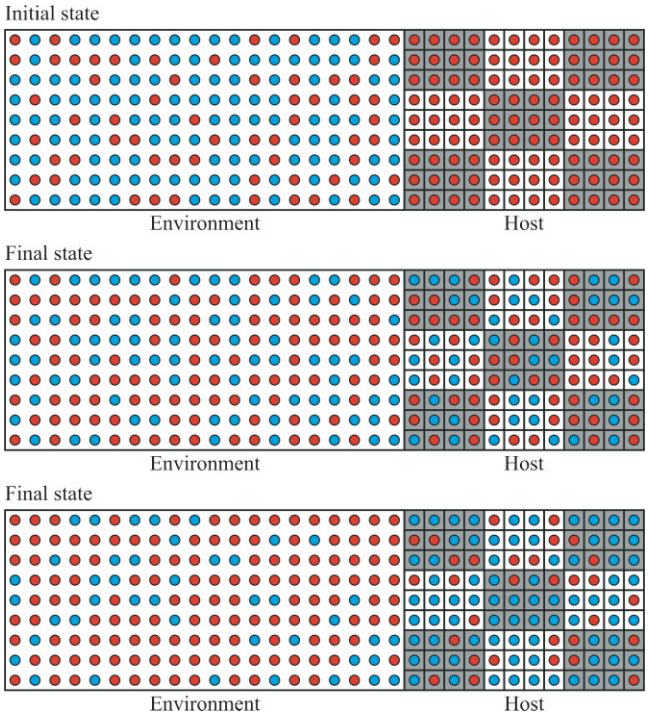

Figure 8. Idealized system, consisting of host (right; every other unit cell is gray-shaded) and environment (left): before the exchange experiment (top) and after establishment of the overall exchange equilibrium (middle). The selectivity of the blue and the red globules is equal for all sites. The same (bottom) after equilibration if the selectivity of the exchanging species (blue) for the host sites is higher than that of the species being exchanged (red; exchange probability: 75%).

Figure 6 shows that the entropy changes of the individual reactions in Equation (17) are shifted in a negative direction with increasing values of r. This is easily proven using Equations (47) and (26) [Eq. (48)]:

$$\frac{d\Delta S(r)}{dr} = R\frac{d\ln K(r)}{dr} = -\frac{R(n_{box}+1)}{r(n_{box}-r+1)} < 0 \quad r \in [1,n_{box}] \tag{48}$$

The course of the $\Delta S(r)$ curve directly visualizes the dependence of the change of mixing entropy occurring in the host in the various exchange reactions on r: By interpreting the curve by means of the particle model and drawing attention to one unit cell, it is seen that, for $r=1$, significant disordering occurs in the unit cell. With increasing values of r, this disordering effect gradually withdraws. For $r=(n_{box}+1)/2$ neither disordering nor ordering occurs. If r grows further, a gradually increasing ordering effect occurs, culminating in a most negative ΔS for $r=n_{box}$.

The reaction entropy ΔS_r of the rth reaction of Equation (17) is the difference in the entropies of the pure, separated products and the pure, separated reactants [Eq. (49)]:

$$\Delta S_r = S(ZA_rB_{n_{box}-r}) + S(B) - S(ZA_{r-1}B_{n_{box}-(r-1)}) - S(A) \tag{49}$$

where $S(B)-S(A)$ is the entropy difference between the two kinds of free cations, including hydration effects. $S(ZA_rB_{n_{box}-r}) - S(ZA_{r-1}B_{n_{box}-(r-1)})$ contains any entropy difference between the two species $ZA_rB_{n_{box}-r}$ and $ZA_{r-1}B_{n_{box}-(r-1)}$. However, since these only differ in one cation, it can be assumed that only contributions related to the exchange of this cation have a share in this entropy-difference term. The only such contributions are the change of inner entropy, described above as a change of mixing entropy, and the entropy difference resulting from hydration differences between A and B in the host.[35] Hence, ΔS_r can be rewritten as Equation (50):

$$\begin{aligned}\Delta S_r &= \Delta S_{r,mix} + S(A(aq_{host})) - S(B(aq_{host})) + S(B(aq)) - S(A(aq)) \\ &= \Delta S_{r,mix} + \Delta S_{AB(aq_{host})} + \Delta S_{BA(aq)})\end{aligned} \tag{50}$$

$\Delta S_{BA(aq)}$ and, because equivalent cation sites are presumed, also $\Delta S_{AB(aq_{host})}$ are independent of r. Summarizing the two terms as $\Delta S_{A,B}$, we get Equation (51):

$$\Delta S_r = \Delta S_{r,mix} + \Delta S_{A,B} \tag{51}$$

We now use these findings to derive explicit formulae for ΔH and ΔS_r.

Using Equations (26) and (51), we rewrite Equation (42) for $r=(n_{box}+1)/2$, which causes $\Delta S_{r,mix}$ to vanish [Eq. (52)]:

$$\Delta H = T\Delta S_{A,B} - RT\ln\left(K_1\frac{n_{box}-\frac{n_{box}+1}{2}+1}{n_{box}\frac{n_{box}+1}{2}}\right) = T\Delta S_{A,B} - RT\ln\left(\frac{K_1}{n_{box}}\right) \tag{52}$$

This result is valid for all reactions in Equation (17). Hence, we can replace ΔH in Equation (47), which yields Equation (53):

$$\begin{aligned}\Delta S_r &= \Delta S_{A,B} - R\ln\left(\frac{K_1}{n_{box}}\right) + R\ln K_r \\ &= \Delta S_{A,B} + R\ln\left(\frac{K_r}{K_1}n_{box}\right)\end{aligned} \tag{53}$$

Hence, we find Equation (54) for the change of free-energy in the rth reaction, as expected.

$$\Delta G_r = -RT\ln K_r \tag{54}$$

We finally derive formulae for the coupled system of the n_{box} reactions of Equation (17). ΔH_{tot} is the n_{box}-fold of ΔH, Equation (55):

$$\Delta H_{tot} = n_{box}T\Delta S_{A,B} - RTn_{box}\ln\left(\frac{K_1}{n_{box}}\right) \tag{55}$$

Using Equation (30), we can also write Equation (56):

$$\Delta H_{tot} = n_{box}T\Delta S_{A,B} - RT\ln K_{tot} \tag{56}$$

ΔS_{tot} is the sum of all ΔS_r [Eq. (57)]:

$$\Delta S_{tot} = \sum_{r=1}^{n_{box}}\Delta S_r = n_{box}\Delta S_{A,B} + R\ln\left(\left(\prod_{r=1}^{n_{box}}K_r\right)\left(\frac{n_{box}}{K_1}\right)^{n_{box}}\right) \tag{57}$$

Using Equations (28) and (30), we find Equation (58):

$$\Delta S_{tot} = n_{box}\Delta S_{A,B} + R\ln\left(K_{tot}\frac{1}{K_{tot}}\right) = n_{box}\Delta S_{A,B} \quad (58)$$

Because of the antisymmetry of the $\Delta S(r)$ function, this result was to be expected. Eventually, we find, from Equations (30), (56), and (58) [Eq. (59)]:

$$\Delta G_{tot} = -RT\ln K_{tot} = -RTn_{box}\ln\left(\frac{K_1}{n_{box}}\right) \quad (59)$$

5. Summary and Outlook

We have described particle distribution and exchange equilibria in a microporous material containing multiple equivalent particle sites. By comparing an exact with an approximate approach to describe particle distribution, we have seen that the approximate approach is perfectly suitable for describing macroscopic systems; while in order to describe individual nanocrystals, the decision as to which approach to use should be taken carefully. As an example, a zeolite A nanocrystal consisting of about 1000 pseudo-unit-cells fixes a lower limit for the use of the approximate particle distribution formula. Simple exact and approximate formulae describing the rational selectivity coefficients of ion-exchange equilibria have been derived on the basis of particle distribution theory. The constancy of rational selectivity coefficients over the whole exchange range is not a principally valid property for describing individual nanoparticles. Instead, these coefficients are only precisely constant in the thermodynamic limit. The minimum size of an ion-exchange system that can be described with the approximate selectivity coefficients can be estimated. A zeolite A crystal, for example, needs to consist of at least one million pseudo-unit-cells. In order to describe ion-exchange isotherms, we have derived a formula formally similar to the Langmuir isotherm. It is valid for ion-exchange systems made up of a variable number of coupled-exchange reactions. Finally, the thermodynamic quantities ΔH, ΔS, and ΔG of the ion-exchange reactions have been discussed. The reasoning is based on a fixed number of particles in the host, that is, we make a canonical ensemble approach. We assume that all cation sites in the host are equivalent. This is clearly in general not true, however, the inequivalence of host sites can be taken into account when experimental data are evaluated.

Theory has been illustrated through its application to zeolite A, treated as a nearly ideal reference system, the only major cut from our ideal model being that the 12 cation sites per pseudo-unit-cell in zeolite A are not strictly equivalent. It was recently applied to ion-exchange experiments performed with zeolite Na-A and zeolite K-A using silver ions as the exchanging species. We found that the presented results can directly be used to evaluate these isotherms, and that it is possible to take the non-equivalence of the particle sites in zeolite A into account.[5]

Acknowledgments

This work was supported by the Swiss National Science Foundation Projects NFP47 (4047-057481) and NF 2000-06/259/00/1.

Keywords: ion exchange · Langmuir isotherm · microporous materials · particle distribution · zeolites

[1] *Host–Guest-Systems Based on Nanoporous Crystals* (Eds.: F. Laeri, F. Schüth, U. Simon, M. Wark), Wiley-VCH, Weinheim, **2003**.
[2] a) G. Schulz-Ekloff, D. Wöhrle, B. van Duffel, R. A. Schoonheydt, *Microporous Mesoporous Mater.* **2002**, *51*, 91; b) S. Hashimoto, *J. Photochem. Photobiol., C* **2003**, *4*, 19; c) K. Ha, Y.-L. Lee, Y. S. Chun, Y. S. Park, G. S. Lee, K. B. Yoon, *Adv. Mater.* **2001**, *13*, 594.
[3] a) G. Calzaferri, C. Leiggener, S. Glaus, D. Schürch, K. Kuge, *Chem. Soc. Rev.* **2003**, *32*, 29; b) C. Leiggener, G. Calzaferri, *ChemPhysChem* **2004**, *5*, 1593.
[4] a) G. Calzaferri, S. Huber, H. Maas, C. Minkowski, *Angew. Chem.* **2003**, *115*, 3860; *Angew. Chem. Int. Ed.* **2003**, *42*, 3732; b) M. M. Yatskou, M. Meyer, S. Huber, M. Pfenniger, G. Calzaferri, *ChemPhysChem* **2003**, *4*, 567; c) S. Huber, G. Calzaferri, *ChemPhysChem* **2004**, *5*, 239; d) S. Huber, G. Calzaferri, *Angew. Chem.* **2004**, *116*, 6906; *Angew. Chem. Int. Ed.* **2004**, *43*, 6738.
[5] M. Meyer, C. Leiggener, G. Calzaferri, *ChemPhysChem* **2005**, *6*, 1071.
[6] T. L. Hill, *Statistical Mechanics: Principles and Applications*, McGraw-Hill, New York, **1956**.
[7] D. M. Ruthven, *Nat. Phys. Sci.* **1971**, *232*, 70.
[8] R. Derrah, K. Loughlin, D. M. Ruthven, *J. Chem. Soc., Faraday Trans. 1* **1972**, *68*, 1947.
[9] D. M. Ruthven, K. F. Loughlin, K. A. Holborow, *Chem. Eng. Sci.* **1973**, *28*, 701.
[10] M. Allen, D. Tildesley, *Computer Simulation of Liquids*, Oxford University Press, Oxford, **1997**.
[11] B. Smit, *Mol. Phys.* **1995**, *85*, 153.
[12] D. M. Razmus, C. K. Hall, *AIChE J.* **1991**, *37*, 769.
[13] R. J.-M. Pellenq, B. Tavitian, D. Espinat, A. H. Fuchs, *Langmuir* **1996**, *12*, 4768.
[14] T. Maris, T. J. H. Vlugt, B. Smit, *J. Phys. Chem. B* **1998**, *102*, 7183.
[15] J. Narkiewicz-Michalek, P. Szabelski, W. Rudzinski, A. Chiang, *Langmuir* **1999**, *15*, 6091.
[16] P. Pascual, P. Ungerer, B. Tavitian, P. Pernot, A. Boutin, *Phys. Chem. Chem. Phys.* **2003**, *5*, 3684.
[17] J. Liu, M. Dong, Z. Qin, J. Wang, *J. Mol. Struct. (Theochem)* **2004**, *679*, 95.
[18] a) C. F. Mellot, A. K. Cheetham, *J. Phys. Chem. B* **1999**, *103*, 3864; b) K. G. Ayappa, *J. Chem. Phys.* **1999**, *111*, 4736.
[19] A. Kunzmann, R. Seifert, G. Calzaferri, *J. Phys. Chem. B* **1999**, *103*, 18.
[20] a) R. Seifert, A. Kunzmann, G. Calzaferri, *Angew. Chem.* **1998**, *110*, 1603; *Angew. Chem. Int. Ed.* **1998**, *37*, 1521; b) R. Seifert, R. Rytz, G. Calzaferri *J. Phys. Chem. A* **2000**, *104*, 7473; c) C. Leiggener, D. Brühwiler, G. Calzaferri, *J. Mater. Chem.* **2003**, *13*, 1969.
[21] G. Calzaferri, D. Brühwiler, S. Megelski, M. Pfenniger, M. Pauchard, B. Hennessy, H. Maas, A. Devaux, U. Graf, *Solid State Sci.* **2000**, *2*, 421.
[22] D. W. Breck, *Zeolite Molecular Sieves*, Wiley, New York, **1974**.
[23] W. Loewenstein, *Am. Mineral.* **1954**, *39*, 92.
[24] J. V. Smith, J. J. Pluth, *Nature* **1981**, *291*, 265.
[25] D. Olson, W. M. Meier, Ch. Baerlocher, *Atlas of Zeolite Framework Types*, 5th Rev., Elsevier Science, Amsterdam, **2001**.
[26] M. M. J. Treacy, J. B. Higgins, *Collection of Simulated XRD Powder Patterns for Zeolites*, 4th Rev., Elsevier Science, Amsterdam, **2001**.
[27] D. W. Breck, W. G. Eversole, R. M. Milton, T. B. Reed, T. L. Thomas, *J. Am. Chem. Soc.* **1956**, *78*, 5963.
[28] T. B. Reed, D. W. Breck, *J. Am. Chem. Soc.* **1956**, *78*, 5972.
[29] P. Lainé, R. Seifert, R. Giovanoli, G. Calzaferri, *New J. Chem.* **1997**, *21*, 453.
[30] J. J. Pluth, J. V. Smith, *J. Am. Chem. Soc.* **1980**, *102*, 4704.
[31] R. M. Barrer, J. Klinowski, *J. Chem. Soc., Faraday Trans.* **1972**, *68*, 73.
[32] M. Meyer, *Ph.D. Thesis*, University of Bern, **2005**.

[33] P. W. Atkins, *Physical Chemistry*, 6th ed., Oxford University Press, Oxford, **1998**.
[34] G. Calzaferri, N. Gfeller, *J. Phys. Chem.* **1992**, *96*, 3428.
[35] The possible change in the number of intracrystalline water molecules per unit cell in the course of the ion exchange does not need to be taken into account here, since the intracrystalline water itself is not a part of the system in this consideration. It is rather treated as a part of the aqueous environment.

Received: March 6, 2005

